Study of Vortex Ring Dynamics in the Nonlinear Schrödinger Equation utilizing GPU-Accelerated High-Order Compact Numerical Integrators

Ph.D. Dissertation Proposal for Ronald M. Caplan

Project Summary

Being the normal form for nonlinear propagation of envelope waves, the nonlinear Schrödinger equation (NLSE) is an ubiquitous equation with diverse applications including light propagation through nonlinear optical media and mean-field dynamics in Bose-Einstein condensates.

One of the most interesting family of solutions to the NLSE are those which exhibit topological charge. In two dimensions, these coherent structures correspond to vortices while, in the more challenging three-dimensional case, they correspond to vortex rings.

Vortex rings are ring-shaped structures which, due to their vorticity, form a toroidal area whose center ring has zero-density, with increasing density away from the center which converges to a constant-density background.

We propose to study the dynamics and interactions of vortex rings in the NLSE. The study will focus on multi-vortex ring interactions. Due to the inherent lack of a close form solution for vortex rings and the dimensionality where they live, efficient numerical methods to integrate the underlying equations have to be developed in order to perform extensive studies of collision scenarios.

To facilitate this, compact high order numerical schemes are developed including new semi-compact boundary conditions. Implementation of the codes is performed on NVIDIA graphic processing unit (GPU) parallel architectures. The codes running on the GPU are many times faster than their serial counterparts, and are much cheaper to run than on standard parallel clusters using programming techniques such as MPI and OpenMP. The codes are developed with future usability in mind, and therefore are written to interface with MATLAB utilizing custom GPU-enabled C codes with a MEX-compiler interface. Reproducibility is achieved by freely providing distributable code packages including user manuals and set-up files.

1 Results from Prior Support

This proposal is closely related to previous work done on bright vortex structures in systems governed by various forms of the nonlinear Schrödinger equation (NLSE), and contains a natural progression of computational tools developed therein. The previous work was performed with support from the Computational Science Research Center (**CSRC**) at San Diego State University, as well as NSF grant **NSF-DMS-0806762**. The results of those studies have lead to two publications, as well as numerous research presentations at professional and academic conferences, symposiums and colloquiums. The studies can be summarized as follows:

a) Modulational Instability of Vortices in the NLSE: Bright vortices in the NLSE are modulationally unstable in the azimuthal direction. We studied the rate of growth and number of filaments in the break up of the vortices. Our goal was to provide information relevant to experimenters pertaining to the lifespan of the vortices. Our theoretical results matched closely with numerical simulations. In the process of the study, an extremely accurate, yet simple, approximate analytical radial profile was formulated through a variational approach which can be used to describe the structure of vortices of arbitrary charge. Fig. 1 shows an example of azimuthal instability, as well as some of the asymptotic profiles and growth rate results. The work resulted in the publication of Ref. [1].

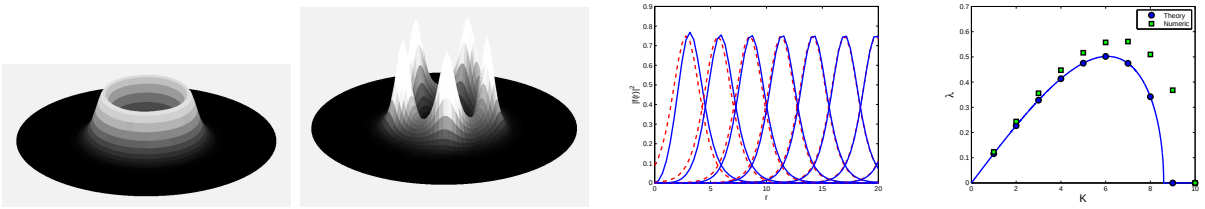

(a) (b) (c)

Figure 1: From left to right: a) Example of modulational instability of a vortex in the azimuthal direction. b) Bright vortex profiles for charges $1-7$ using the approximate analytical profile (dashed lines) and comparison to the numerically-exact profiles (solid lines). c) Theoretical growth rates for unstable azimuthal modes and comparison to direct simulations.

b) Stability and Scattering of Vortices in the Cubic-Quintic NLSE: Unlike the bright vortices in the NLSE, when realized in the cubic-quintic NLSE, such vortices can be stable. We studied the stability bounds in terms of a critical frequency, and compared our theoretical results with those done by other researchers as well as our own simulations. We also studied the growth rates and number of break-up filaments in the vortices above the critical stability frequency. Our results matched simulations well and, as in the NLSE case, we developed an extremely accurate analytical approximation to the vortex profiles. In addition, we confirmed the existence bounds (in terms of frequency) of the vortices and, through variable-precision numerical computations, were first to create vortex profiles for high frequencies very near the existence bound. The study was then extended to include dynamics of collisions of stable vortices, and their scattering. Fig. 1 shows examples of high-frequency vortex profiles, growth rate results of unstable vortices, an illustration of the stability threshold of a vortex, and an example of vortices in collision. The project resulted in the submission of Ref. [4].

c) Simulating the one-dimensional NLSE using NVIDIA GPUs with MATLAB and

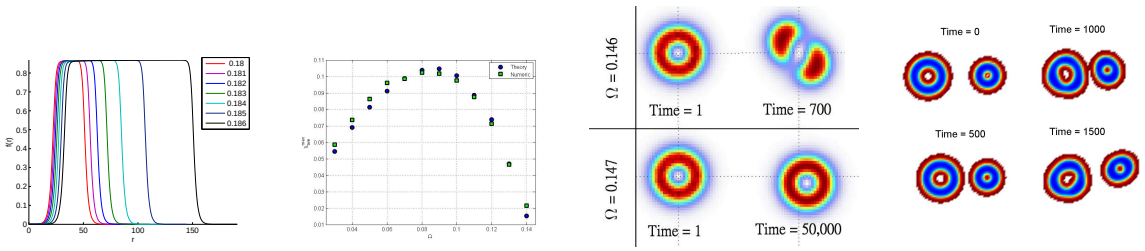

(a) (b) (c) (d)

Figure 2: From left to right: a) Numerically-exact bright cubic-quintic unitary charge vortex profiles near the critical existence frequency. b) Theoretical growth rates for unstable azimuthal modes and comparison to direct simulations. c) Example of the stability of a unitary charge vortex above the critical frequency. d) Example of stable charge 2 and charge 1 vortices undergoing a near-elastic collision.

CUDA: A new advancement in parallel computation is the use of graphical processing units (GPUs) for computational problems. As a project for a seminar in the CSRC, we developed an integration code using NVIDIA's compute unified device architecture (CUDA) application programming interface (API) to simulate the one-dimensional NLSE. For ease of use, the codes were written to interface with MATLAB. Using a GPU card with a price of approximately $200, we achieved speedups of over sixty times (for large-grid problems) when compared to an equivalent serial code. The study opened new ground in the possibilities of efficient and inexpensive simulations of the NLSE.

The results above have given us much insight into vortex solutions to the NLSE, as well as expanded and refined many computational challenges in the numeric study of such systems. Many of the methodologies, knowledge, and code production developed in these studies will be directly relevant and essential in the proposed project.

2 Background

The NLSE is a universal model describing the evolution and propagation of complex filed envelopes in nonlinear dispersive media. As such, it is used to describe many physical systems including the evolution of water waves, nonlinear optics, thermodynamic pulses, nonlinear waves in fluid dynamics, and waves in semiconductors [12].

One of the most relevant applications with regards to this proposal is the simulation of the dynamics of Bose-Einstein condensates (BECs) of dilute gases [18]. BECs are a state of matter where a collection of bosons, whose de-Broglie wavelengths become comparable to their mean separation distance, undergo a phase transition so that a significant fraction of the bosons find themselves in the same quantum state. In such a case, the collection of bosons behave as one large near-macroscopic coherent particle. In the case of dilute gases, a BEC is formed by cooling the gas to extremely low temperatures (on the order of 10^{-7}K) which lowers the momentum of each atom, causing their de-Broglie wavelength to increase. In such a BEC, the gas cloud behaves as one very large, near-macroscopic atom which can be described by a mean-field approximation (where only two-body collisions are considered, and such collisions are considered to be felt only locally) by the NLSE with appropriate parameters. BECs have also been realized in other bosonic systems such

as magnons in ferromagnetic magnets [13], polaritons in semiconductors [14], and recently, photons within an optical cavity [15].

The atoms in a BEC of a dilute gas can either be attracted to each other in near-collisions, or be repelled. Since in most situations, attractive BECs are unstable and collapse into what is known as a 'Bosenova' [16, 17], most experiments use repulsive atoms, in which case the BEC must be confined by an external trap which is typically realized by magnetic and optical potentials. In such situations, the mean-field dynamics of the BEC can be described using the Gross-Pitaevskii equation which is a NLSE with the added external potential term.

The advisor of the proposed project is currently involved in numerous studies of the dynamics of BECs, and has many publications (including a book) [1]–[11] describing the dynamics of topologically interesting nonlinear wave phenomena. Several other key collaborators are studying similar dynamics in the NLSE, but focused on nonlinear optical applications [19].

While most research done using the NLSE is in the specific application being studied such as those mentioned above, the approach used in our previous studies and proposed in this project is to first study the relevant dynamics and structures in the simplified case of a general form of the NLSE. This allows the results and codes developed from this study to be directly relevant to a much wider group of researchers, thus increasing its impact. The form of the NLSE we use in the proposed study is

$$i\Psi_t + a\,\nabla^2\Psi + V(\mathbf{r})\,\Psi + s\,|\Psi|^2\,\Psi = 0, \tag{1}$$

where Ψ is the wavefunction, a and s are arbitrary parameters, and $V(\mathbf{r})$ is the external potential function. The parameter s represents the local nonlinear interaction response and its sign determines if the NLSE is attractive ($s > 0$) or repulsive ($s < 0$). The modulus-squared of the wavefunction, $|\Psi|^2$, represents the observable which, in the case of BECs, is the boson density, while in nonlinear optic settings, is the intensity of the light. In most of the project, we will assume that there is an infinite constant-density background, and thus the external potential term is set to zero (although it is included in the developed codes). This raises the potential for obtaining analytical results, and allows for simplified dynamics to be studied as interactions with the external potential are ignored. The knowledge gathered can then be extended into specific applications or more complicated modifications of the NLSE. As an example, our previous work on modulational instability of vortices in the cubic NLSE laid the framework to be able to study the more complicated stability and dynamics of vortices in the cubic-quintic NLSE which has closer direct relevance to application (in this case, nonlinear optics).

One of the most interesting family of solutions to the NLSE are those which exhibit topological charge. In two dimensions, these coherent structures correspond to vortices while, in three-dimensions, they can correspond to vortex rings. Vortex rings are ring-shaped structures which, due to their vorticity, form a toroidal area whose center ring has zero-density, with increasing density away from the center which converges to a constant-density background. They have an intrinsic transverse velocity due to their vorticity [21], which can be overcome by considering the vortex rings in a co-moving reference frame, or by counteracting the velocity by a trapping potential [33].

Vortices have been observed in many experiments in quantum systems including BECs and nonlinear optics (see Ref. [20] for an extensive list of studies). Vortex rings have been seen experimentally in super-fluid helium [22] as well as in the context of BECs in the decay of dark solitons in two-component BECs [23] as well as direct density engineering [24, 25, 26]. Numerical studies of experimentally obtainable vortex-ring generation in BECs have also been explored in the context of collisions of multiple BECs [8, 9], flows past an obstacle [6], collapse of bubbles [27], evolution

of rarefaction two-dimensional pulses [28], flow past an ion [29], and dragging of an object through a BEC [30].

The structure and energy of a single vortex ring in the NLSE has been studied analytically [21, 31] with focus on the structure, energy and transverse velocity. The velocity results have been numerically verified in more recent studies [40] although the details of the comparisons were not shown.

Numerical studies directly focused on the structure and stability of vortex rings in trapped BECs have also been done. These include the generation of a steady-state vortex rings [32, 33, 34], multiple parallel ring stuctures [35], and bending-wave instability of vortex rings [36] and their degeneration into quantum turbulence [37]. Some dynamics of vortex rings in trapped BECs have been explored, such as their oscillatory motion resulting in self-annihilation [38], and collisions of vortex rings and solitons in cylindrical BECs [39].

Collisions between numerous vortex rings in an infinitely-large BEC (requiring no external potential) is of main interest in this project. A previous study of such collisions was performed in Ref. [40], but for only a few configurations, and without quantitative analysis. An extensive dynamical study was not done most likely due to the large computational cost of the three-dimensional simulations at the time (typically hours long). The techniques developed and utilized in the proposed project will eliminate that obstacle and allow for a more thorough study of a multitude of collision scenarios.

Bright vortex rings in attractive BECs are also possible to realize, in which case the vortex ring resembles a smoke-ring in that it has a well-defined radius of greatest density which trails off to zero. However, as the analogous two-dimensional bright vortices are unstable and collapse, these bright vortex rings will also undergo such collapse (this has been numerically verified by the PI). As such, its study is not as relevant as the dark vortex rings for repulsive BECs, but for completeness the proposed project will briefly explore even these bright rings (which, in an extension to the cubic-quintic NLSE may be stable for some parameter ranges).

3 Specific Mathematical and Computational Proposal Aims

We now detail what the funding of the present proposal should enable us to achieve:
(1) The project will mathematically describe the structure and dynamics of vortex rings in the three-dimensional NLSE, including deriving asymptotic analytical approximations of the vortex ring structure.
(2) To produce explicit high-order compact finite difference schemes to integrate the NLSE in one-, two- and three-dimensional settings implementing new boundary conditions suited well for the case of constant density backgrounds.
(3) Implement the formulated numerical schemes into codes written in C which run on NVIDIA GPUs using the CUDA API in order to greatly speed up computations at low cost.
(4) Integrate the CUDA codes with MATLAB to allow ease of use for future researchers as well as allow accessible reproducibility of numerical results. MATLAB driver scripts incorporating visualizations, optimizations, and analysis will also be included. A code package will be made available online on a dedicated webpage, complete with straightforward setup guides and installation files.
(5) A major goal and main motivation of the project will be to use the aforementioned code to conduct a thorough study of the dynamics of vortex rings in the NLSE. This will include single

ring structures and their dynamics, and multi-ring interactions including collisions and flybys.

4 Detailed Analysis: Proposed Studies and Preliminary Results

The following is a detailed account of the current status and future work in the proposed study:

4.1 Review of Solitons and Vortices in the NLSE

The three-dimensional vortex rings are a topological extension of two-dimensional vortices whose radial profiles resemble one-dimensional dark solitons. A co-moving dark soliton solution to the NLSE is given by

$$\Psi(x,t) = \sqrt{\frac{\Omega}{s}} \tanh\left[\sqrt{\frac{\Omega}{2a}}\,(x - c\,t)\right] \exp\left(i\left[\frac{c}{2a}\,x + \left(\Omega - \frac{c^2}{4a}\right)t\right]\right). \tag{2}$$

where c is the co-moving velocity and Ω is the frequency. Due to the similarities of lower-dimensional structures to vortex rings, a compilation of prior results is being developed as a resource to describe the vortex rings mathematically as much as possible.

The review covers the most basic properties and dynamics (including stability) of solitons and vortices in one- and two-dimensional settings gleaned from various sources. Because vortex rings are direct extensions of dark vortices, they are of special interest. This is because the dynamics of vortex rings can be compared and related to the dynamics of multiple dark vortices in two dimensions since an axisymmetric cut of a vortex ring is qualitatively equivalent to two opposite charge vortices separated by a distance twice the vortex ring radius.

The general form of two-dimensional vortices is $\Psi(r,\theta,t) = f(r)\exp(i\,(m\,\theta + \Omega\,t))$, where m is the charge of the vortex. Inserting this form into the NLSE yields the time-independent PDE

$$-\left(\Omega + \frac{a\,m^2}{r^2}\right) f(r) + a\left(\frac{1}{r}\frac{df}{dr} + \frac{d^2 f}{dr^2}\right) + s\,f^3(r) = 0. \tag{3}$$

One of the more general and useful results of our previous study on bright vortices was the analytic approximation to the vortex structure which was asymptotically exact for large charge. A similar profile result has been found in the dark vortex case [7] by an asymptotic analysis of Eq. (3), yielding the radial profile

$$f(r > 0) \approx \mathrm{Re}\left(\sqrt{\frac{\Omega}{s} + \frac{a\,m^2}{s\,r^2}}\right). \tag{4}$$

These profiles are very useful as initial ansatze to nonlinear optimization routines, in order to get numerically exact solutions. In Fig. 3, a dark soliton in the one-dimensional NLSE is shown, along with several two-dimensional dark vortex profiles and an example of a dark vortex.

4.2 Mathematical Structure of Vortex Rings

As mentioned in the previous section, it was possible to derive asymptotic analytic structures for vortices in two dimensions. We would like to extend that to the vortex rings as well. Although the vortex rings do not have the symmetry necessary to reduce to a one-dimensional profile, in the limit

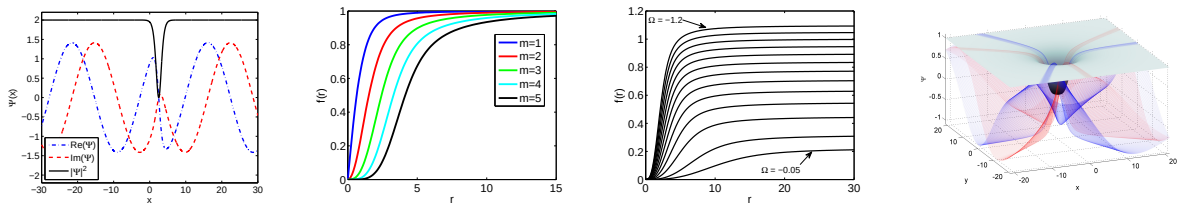

(a) (b) (c) (d)

Figure 3: From left to right: a) One-dimensional co-moving dark soliton solution to the NLSE given by Eq. (2). b) Two-dimensional dark vortex profiles of frequency $\Omega = -1$ and charges $m = 1$–5. c) Dark vortex profiles for charge $m = 3$ and frequencies $\Omega \in [-0.05, -1.2]$. d) A charge $m = 3$, frequency $\Omega = -1$ dark vortex showing the density ($|\Psi|^2$) in gray, Re(Ψ) in blue mesh, and Im(Ψ) in red mesh.

as the vortex ring radius d gets large, the vortex ring cross-section becomes nearly symmetric about its polar axis. As such, asymptotic profiles may be able to be derived that can assist optimization routines converge to the desired solution.

Unlike the two-dimensional vortices, vortex rings have an inherent velocity perpendicular to their axis of rotational symmetry due to Helmholtz's vortex law [41]. Thus, vortex rings in a constant-density background do not have a steady-state solution, but rather a co-moving steady-state solution. It can be shown that a steady-state solution to the NLSE co-moving in the z-direction with velocity c has the form [42]

$$\Psi(x, y, z, t) = e^{i\rho(z,t)}\, U(x, y, Z),$$

where

$$\rho(z, t) = \frac{c}{2a}\, z + \left(\Omega - \frac{c^2}{4a}\right)\, t + \phi,$$

and ϕ is an arbitrary phase shift, $\Omega < 0$ is the frequency, $Z = z - c\,t$, and $U(x, y, Z)$ solves the time-independent PDE

$$-\Omega\, U + a\nabla^2 U + s|U|^2 U = 0.$$

We can thus write a 'steady-state' vortex ring solution (with an added back-flow) in cylindrical coordinates as

$$\Psi(r, z, \theta, t) = g(r, z) \exp\left[i\left(\Omega\, t + m\, \phi(r, z; d) - \frac{c}{2a}\, z\right)\right], \tag{5}$$

where m is the charge of the vortex ring, d is the radius of the ring, and $\phi(r, z; d) = \arctan(z/(r-d))$. When Eq. (5) is inserted into the NLSE, one gets the time-independent PDE

$$-\left[\Omega + \frac{c^2}{4\,a} + \frac{a\,m^2}{\rho^2} - (r-d)\frac{m\,c}{\rho^2}\right]\, g + a\left[\frac{1}{r}\, g_r + g_{rr} + g_{zz}\right] + s\,|g|^2\, g + \tag{6}$$
$$i\,\frac{2\,a\,m}{\rho^2}\left[(r-d)\; g_z - z\left(g_r - \frac{1}{2\,r}\, g\right)\right] - i\,c\,g_z = 0,$$

where $\rho^2(r, z; d) = (r-d)^2 + z^2$. We plan to use numerical optimization routines to find steady-state solutions to Eq. (6) in order to get numerically-exact solutions for the initial condition of a

co-moving vortex ring. One difficulty is that one must know the velocity to get the correct co-moving solution. Fortunately, the velocity is known analytically (up to two asymptotic terms) as described in Ref. [21]. In the general parameters of Eq. (1) the velocity is

$$c \approx -\frac{a\,m}{d}\left[\ln\left(8\,d\sqrt{\frac{-\Omega}{a}}\right) - 0.615\right]. \tag{7}$$

Preliminary simulations of the vortex rings show that this velocity is extremely accurate, and thus can be used to obtain the numerically-exact vortex rings.

4.3 High Order Compact Numerical Schemes

The proposed study of vortex ring dynamics will require many three-dimensional simulations with fairly large resolution. In order to reduce the grid size required, we want to use higher-order numerical schemes. Such schemes allow one to simulate a solution with the same accuracy as a second-order scheme, but with many fewer grid points. In fact, typically, when using higher order schemes, the grid size requirement becomes dependent on being able to resolve the structure of the solution, and not on the accuracy involved in the computation.

Higher-order finite difference schemes are typically achieved by computing a wider stencil, that is, using more points away from the computed point to calculate the derivatives. This adds a difficulty near the boundary, as one must be able to calculate the inner point near the boundary with the same accuracy as the internal scheme. If this is not done, the entire simulation will eventually become lower-order. Implementing the boundaries to the desired order can be complicated to implement. Another disadvantage of wide-stencils is that they cause many parallel implementations to be more difficult to realize, as different compute nodes must share or transfer more boundary values to their neighboring nodes [43]. Besides the added complexity of the codes, the extra communication/global-memory-access slows down the parallel performance.

For the aforementioned reasons, many code developers have showed great interest in high-order compact (HOC) schemes. These are finite-difference schemes which exhibit higher order accuracy but still only rely on the neighboring points to compute spatial derivatives. HOC schemes have been developed for various steady-state equations [44]–[47], as well as time-dependent PDEs [48, 49] including the NLSE [50]–[53]. The time-dependent HOC schemes developed so far are all implicit (even if the time-stepping is done with an otherwise explicit scheme), requiring solving a large linear system each time step, as well as iterative processes (when simulating nonlinear PDEs such as the NLSE). Implicit schemes in general are very difficult to optimally parallelize, and we therefore want to develop HOC schemes that are *fully explicit*.

In order to use a HOC scheme and still keep the overall scheme explicit, we formulate a two-step procedure in computing the spatial derivatives, where each individual step is a compact computation. This two-step HOC (2SHOC) scheme is then combined with fourth-order Runga-Kutta (RK4) time-stepping. The first step of the 2SHOC scheme computes the standard second-order finite difference approximation to the derivatives of the Laplacian, while the second step uses these precomputed derivatives to compactly approximate the fourth-derivative truncation term in the second-order finite difference of the Laplacian. An example of the 2SHOC scheme in two dimen-

sions is given by

$$
\begin{aligned}
&1) \quad D_{i,j} = \frac{1}{h^2} \begin{array}{|c|c|c|}\hline & 1 & \\ \hline 1 & \text{-4} & 1 \\ \hline & 1 & \\ \hline \end{array} \Psi_{i,j} \\
&2) \quad \nabla^2 \Psi_{i,j} \approx -\frac{1}{12} \begin{array}{|c|c|c|}\hline & 1 & \\ \hline 1 & \text{-12} & 1 \\ \hline & 1 & \\ \hline \end{array} D_{i,j} + \frac{1}{6h^2} \begin{array}{|c|c|c|}\hline 1 & & 1 \\ \hline & \text{-4} & \\ \hline 1 & & 1 \\ \hline \end{array} \Psi_{i,j},
\end{aligned}
\tag{8}
$$

where h is the step size of the spatial grid.

The formulation of the 2SHOC scheme Laplacian operator has been worked out in one-, two-, and three-dimensional settings, and tested successfully for fourth-order spatial accuracy. In multi-dimensional settings, there are two formulations of the scheme, one which uses more memory space but requires less computations, and another that uses more computations, but requires less memory space. A computational and memory analysis comparing the two 2SHOC schemes to each other, as well as comparing them with the standard fourth-order wide-stencils has been done analytically, but further work is planned in order to confirm the results numerically.

A disadvantage of using explicit schemes is that they are typically conditionally stable, meaning that the time step size is bounded by the spatial step, whereas implicit schemes are typically unconditionally stable [54]. Due to the conditional stability, in order to get the best performance of the 2SHOC scheme, the stability bounds should be known to avoid taking unnecessarily small time steps. Linear stability bounds are straightforward to obtain [55], but the effects of the nonlinear terms in the NLSE are not trivial and need to be explored. Some of the nonlinear stability results in one-dimension have been realized, but more work is needed to be able to have stability bounds for various boundary conditions and for the two and three-dimensional schemes. The compiled results of the stability analysis will be formulated into a write-up to be distributed online as a resource for those using the method.

The formulation of the 2SHOC schemes, and their use in simulating the NLSE is currently being compiled into a paper to be submitted to the journal of Applied Mathematics and Computation [2].

4.4 Modulus-Squared Dirichlet Boundary Condition

In almost all numerical simulations, proper handling of boundary conditions (BCs) can be quite challenging. Sometimes an otherwise stable scheme will become unstable depending on how BCs are computed. In addition, high-order schemes can degrade in accuracy to lower-order when using lower-order BCs.

Most often, researchers will use tried-and-true boundary conditions which are very simple yet provide desirable results. One of the most common is the use of Dirichlet boundary conditions. This is where one sets the boundary of the simulation to a constant value at each time step. In may applications, this value is set to zero, as many solutions of interest have decaying tails which rapidly tend towards zero. In NLSE simulations of BECs, the external potential term makes all BECs tail off towards zero at the boundaries, in which case Dirichlet BCs can be used.

As mentioned in Sec. 2, in the proposed study, we will mainly focus on simulating the NLSE without an external potential, in which case our domain is an infinite constant density background.

Since the density is defined by the modulus-squared of the wavefunction, standard Dirichlet conditions cannot be used since the real and imaginary parts of the wavefunction oscillate constantly due to the intrinsic frequency of the system and the dynamics of the solutions. To avoid this problem, we have developed a new Modulus-Squared Dirichlet (MSD) BC which simulates a constant-density at the boundaries. The BC is derived by assuming the modulus-square of the wavefunction is constant-valued at the boundary, separating the real and imaginary parts of the wavefunction, taking time-derivatives of the resulting equation, and then solving for a general solution of the resulting coupled differential equation along with taking one-sided spatial differences. The resulting MSD BC is described as:

$$\left.\frac{\partial \Psi}{\partial t}\right|_B \approx \left(\frac{\Psi_B}{\Psi_{B-1}}\right) \left.\frac{\partial \Psi}{\partial t}\right|_{B-1}, \tag{9}$$

where the subscripts B and $B-1$ refer to the boundary point and the interior point normal to the boundary respectively.

The MSD BC relies only on the nearest interior point normal to its surface, making the MSD quasi-compact (it is not truly compact because the interior point's time-derivative must be calculated first, which will often rely on other interior points). It can also be used in multidimensional settings with ease, and also can be used for any time-dependent complex PDE.

The MSD BC has been implemented in all our codes, and tests are underway to see how it compares to alternative BCs in terms of accuracy, stability, and conserved quantities (such as mass and energy). We also plan to test the MSD in higher-dimensional settings with vortex solutions to see how the MSD BC handles the phase and vorticity of the solutions near and at the boundary versus other easy-to-implement BCs. Preliminary results show that for solutions which become flat near the boundaries, using a zero-Laplacian BC is slightly more accurate and conserves quantities better than the MSD, but for other solutions, the MSD seems to be the only simple-to-use BC that is stable, proving its robustness. See Fig. 4 for an example of such a scenario.

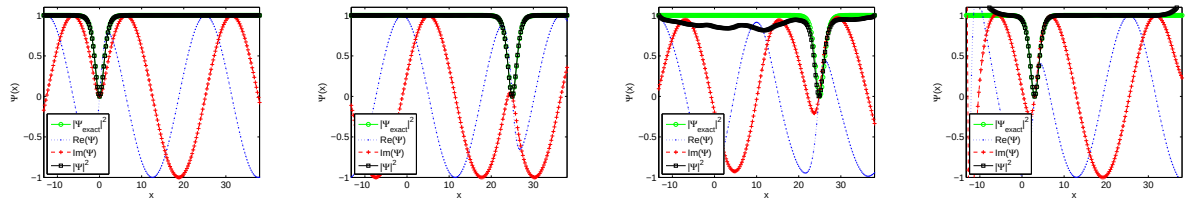

(a) (b) (c) (d)

Figure 4: From left to right: a) Initial condition of a one-dimensional co-moving dark soliton given by Eq. (2). b) Snapshot of simulation at time $t = 50$ using the MSD BC. c) Snapshot of simulation at time $t = 50$ using a $\nabla^2\Psi = 0$ BC. d) Snapshot of simulation at time $t = 6.5$ (when simulation crashed) using a one-sided differencing BC.

The derivation of the MSD BC and results obtained from the numerical tests will be included in a paper to be submitted to the journal of Applied Mathematics and Computation [3].

4.5 Multi-Dimensional GPU-Accelerated NLSE Integrators

Although using higher order numerical schemes can make running large simulations more efficient, for the proposed project this is not enough. In order for the project to be completed in the

allotted time, further methods of improving code performance must be used. The most common way to decrease computation time is to develop codes which run on parallel systems consisting of multiple CPUs using MPI and/or OpenMP. However, a relatively new form of parallel computing has emerged as a low-cost and efficient means to speed up codes. Graphical processing units (GPUs) were first developed in order to allow graphics cards to parallelize their massive computations to speed up video games and image processing. It was then realized that such hardware could be adapted to run scientific codes as well. This led to the development of code APIs which allows one to write code which takes advantage of the GPU hardware. Nvidia cooperation is the leading company in this new form of computing, developing the compute unified device architecture (CUDA) API which can be compiled to run scientific codes on Nvidia's line of GPU video cards, as well as non-video stand-alone GPUs designed specifically for parallel computation.

For many problems, GPU computing is seen as a large improvement over previous parallel techniques. A typical GPU (as of this writing) can have up to 512 processing cores and up to 6GB of RAM, which allows a maximum throughput of over a Tera-FLOP on a single card. The price of the GPUs is another major factor, as one (as of this writing) can purchase an off-the-shelve GPU with over 400 cores, and 1-2GB of RAM for under $450. This allows super-computing capabilities to be realized on a single desktop PC.

A concern that has arisen in the use of GPU computing is the issue of portability. If one writes code using CUDA, that code will only run on Nvidia brand GPUs. In response to this potential problem, an API called OpenCL was created which can be run on multiple brands of GPUs, as well as on standard CPU clusters. The OpenCL API is much more abstract in structure to allow it to be compatible with many systems and therefore more portable. However, using OpenCL on Nvidia GPUs decreases performance when compared to using CUDA [57]. We therefore use CUDA in our codes and note that the native CUDA C code is similar enough in structure, that porting a CUDA code to OpenCL would not be too difficult if future developments required it.

The proposed project will include utilizing GPU computing to increase the speed of the implementation of our numerical schemes into NLSE integrator codes. As previously mentioned, since the numerical methods are compact, the parallel implementation is easier to write than wide-stencil schemes. The codes developed are written in CUDA's native C language, and non-CUDA equivalent codes in C are also produced for speed comparisons. Standard second-order central-difference codes are also included. CUDA implementations of finite difference schemes for various equations have been tested with good results [58]–[61]. However, high-order finite difference schemes were not produced, nor have CUDA codes been written specifically for the NLSE.

As mentioned in Sec. 1, in our previous work, we successfully produced a one-dimensional NLSE integrator using CUDA and tested its performance. Maximum speedups of over 60 times were achieved. Since this time, the development of two and three-dimensional codes has been underway. Also, a brand new family of CUDA GPU card architecture (Fermi) with an impressive set of improvements [56] has been released and our codes have been altered to take advantage of the new developments.

The codes have been tested successfully for consistency, and a thorough study of their speedups is planned. Preliminary results show that for a typical three-dimensional simulation of vortex rings in the NLSE, speedups of over a factor of 16 have been observed when compared to new dual-thread CPUs (the speedup compared to older CPUs is over 32). New tests of one and two-dimensional simulations are planned, as these have not yet been tested on the new Fermi GPUs. Before running the final speedup results, we plan to further optimize the codes in order to try to

get the best possible efficiency for use with our simulations. Fig. 5 shows timing results of the three-dimensional CUDA codes compared to a CPU.

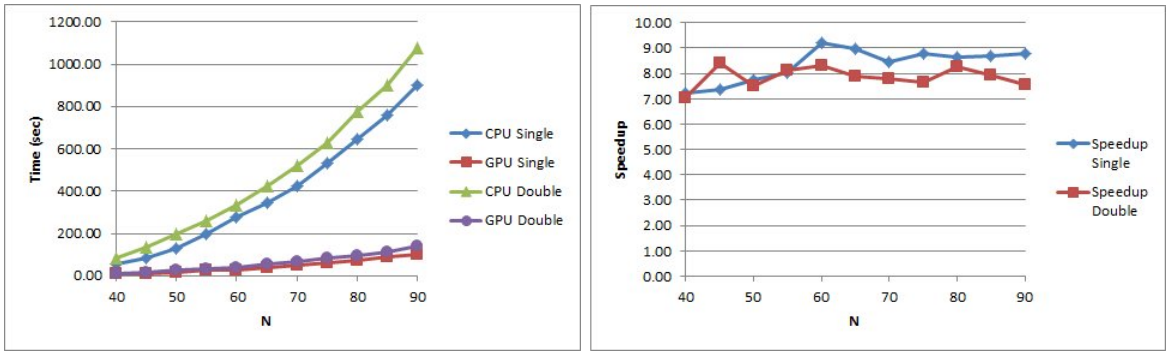

Figure 5: Timing results for a three-dimensional NLSE simulation over 6370 time steps using both single and double precision. N is the dimension of the grid ($N \times N \times N$). In this test a best speedup of around 9 is observed.

A cost-analysis is also planned, studying the price versus speedup of the GPU codes versus other parallel implementations. This is important as writing code for GPUs requires a non-trivial learning-curve and is different from other parallel code APIs. This means that older codes cannot necessarily be converted into GPU codes but may need to be re-written from scratch. Therefore, a cost-analysis is vital for researchers to make decisions on whether to use GPU acceleration or not.

4.6 MATLAB Code Implementation

MATLAB is a mathematical computational software program created by MathWorks Inc. It has become a standard in many academic institutions as well as in industry for mathematical computations. However, there is a prevalent opinion that while MATLAB may be useful for course work, small-scale codes, and learning purposes, for serious calculations it is simply too slow to be useful. In the proposed project we will show that this is not the case, and as such, one can take advantage of all the benefits and ease of using MATLAB while still running large efficient codes. This makes numerical studies much more efficient as visualizations, formation of initial conditions, optimizations, and analysis of data become much easier to implement.

The way to achieve efficient large-scale codes in MATLAB is to write custom C codes which connect to MATLAB through an interface compiler called MEX. Once the C codes have been written to be MEX-compatible and compiled, they can be called from a MATLAB script directly. The codes run as fast as an equivalent stand-alone C code, with minimal overhead, and are up to 10 times faster than the equivalent script codes.

Since the native language for GPU-compatible CUDA codes is C, adding GPU functionality to MATLAB is in theory straightforward (however setup can be difficult, an issue discussed below). The newest versions of MATLAB have GPU-compatibility built-in, and ways to compile CUDA C code segments into callable functions. However, because many researchers do not have the newest versions of MATLAB, in the interest of portability, it is preferable to not use these built-in functions, but rather write C codes which contain CUDA code directly, and compile them with a CUDA-capable MEX compiler called NVMEX. Further portability is maintained in this manner by noting that besides the initial MEX interface in the C codes (which gives the code access to

the MATLAB input parameters and data), the codes are written in generic C and CUDA C code, which can easily be exported to a purely C code if desired.

The proposed project will include the development and distribution (on a dedicated web site) of our completed CUDA MEX codes including MATLAB script files which call the CUDA-enabled integrators for the NLSE in one, two, and three dimensions. The script files will have built-in visualizations and analysis tools. All codes will be thoroughly commented and organized for ease of use. Due to the fact that setting up CUDA-MEX files and compiling them can be tricky (especially on Windows systems), we will also provide simple-to-follow set-up guides and installation files along with the codes. In addition, we will provide a large variety of pre-compiled binaries for those who do not want to take the time to compile the codes directly. The code package will be named NLSEmagic (**NLSE** **M**ultidimentional M**A**tlab-based **G**PU-accelerated **I**ntegrators using **C**ompact high-order numerical schemes) and distributed on `http://www.nlsemagic.com`. A preview image of the website is shown in Fig. 6.

Figure 6: Preview of the website for distributing the NLSE codes.

Currently, many of the codes are completed, with large script driver codes which can reproduce our research results (including order tests for the 2SHOC scheme, boundary-condition test, and CUDA timings). The scripts use other freely available script files for visuals (vis3D, quiver2) and optimizations (nsoli). Our scripts are quite large, and therefore we plan to create a streamlined version of the files with basic functionality for inclusion in the NLSEmagic package. The full research script codes will also be provided as a means of ensuring reproducibility in the results of the research (a topic of much interest in the computational science community [63]).

4.7 Single Vortex Ring Structure and Dynamics

Most previous studies of vortex rings in BECs use steady-state solutions where the rings are held stationary by the external potential. These vortex rings can be numerically found by running an approximate guess for the vortex ring in imaginary time integration [33] to converge to the steady-state solution. However, in the current study, we wish to use co-moving vortex rings in an infinite density background. Previous studies [40] in this setting have used approximate vortex rings, and due to their stability properties, allowed the discrepancies in the structure to be shed off as noise in the simulations. This noise was considered small enough not to adversely effect the dynamics in a major way.

In order to more carefully study the dynamics of vortex ring collisions, we wish to limit the noise from the solutions as much as possible. We therefore seek numerically-exact co-moving vortex rings solutions. Our plan is to seed an approximate axisymmetric cut of a vortex ring into Eq. (6) [where

the velocity c is computed from Eq. (7)] and use numerical optimization routines [62] to converge to the numerically-exact solution. As this will necessitate full two-dimensional optimizations, we will seek the most efficient routines, especially ones which do not require the formation of the full Jacobian matrix (which can often be too memory intensive).

To obtain the approximate axisymmetric cut of a vortex ring, we will use a numerically-exact two-dimensional dark vortex. This is achieved by seeding the approximate profile of Eq. (4) into the radial time-independent PDE of Eq. (3) and using a one-dimensional numerical optimization routine to find the numerically exact solution.

Once the numerically exact vortex rings are found, we plan to run a series of simulations tracking their radius and velocity numerically, and compare the results to the analytic predictions. Also, noting that an axisymmetric cut of a moving vortex ring looks qualitatively equivalent to two two-dimensional vortices of opposite charge moving in parallel (due to their vorticity), we will compare the velocity versus radii of the vortex rings to the two-dimensional equivalent scenario. Preliminary results show that the vortex ring velocity is faster than the two-dimensional vortices by a factor of about four.

Further single ring simulations will perturb the rings in specific ways to induce quadrupole oscillations and track their frequencies. This will be accomplished by fitting (using a least-squares approach) to the magnitude of the vorticity of the vortex ring, a three-dimensional function describing a one-dimensional ring with a tailing Gaussian density profile with various parameters. Fig. 7 shows a vortex ring and some snapshots of a vortex ring undergoing quadrupole oscillations.

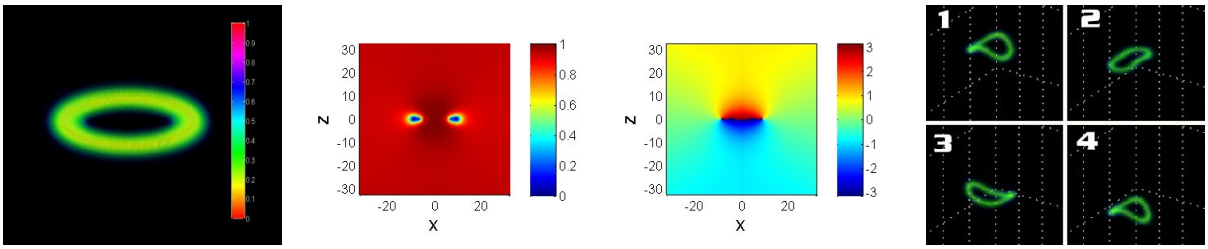

(a) (b) (c) (d)

Figure 7: From left to right: a) Volumetric rendering of the density of a vortex ring of radius $d = 7$ in the NLSE. b) Two-dimensional cut in the x–z plane of the density of the vortex ring. c) Two-dimensional cut in the x–z plane of the phase of the vortex ring. d) Example of quadrupole oscillations of a vortex ring.

Finally, vortex rings with larger than unitary charge will be explored. Preliminary results show that the rings break up into multiple rings of unitary charge very quickly, leading to interesting multi-ring interactions.

4.8 Multiple Vortex Ring Interactions

The most interesting dynamics of vortex rings occur when numerous rings interact. The proposed project seeks to study numerous collisions and interaction scenarios. Other researchers have done an initial study of some two-ring collisions [40]. We seek to greatly expand on those results using numerically-exact vortex rings, and many more interaction configurations. We split our study into collisions/interactions in axisymmetric and non-axisymmetric settings.

Axisymmetric configurations to be explored include two opposite charge vortex rings in direct collisions which then annihilate (as seen in Ref. [40]), as well as when two rings of opposite charge but different radii collide. Equal charge vortex ring interactions will also be studied, which in preliminary simulations show the rings in a loop-the-loop pattern traveling at an approximately constant velocity with one ring shrinking in radius and passing through the other ring, and then the radius increasing, while the other vortex ring's radius shrinks and passes through the first ring and so on. This pattern repeats itself as the pair of rings travels in the z-direction. We will study the long-term stability of this scenario as well as how the scenario changes with different vortex radii. Another axisymmetric configuration we plan to study is that of multiple stacked vortex rings of equal or opposite charge with various radii.

In all axisymmetric configurations studied, we plan to compare the vortex ring dynamics along an axisymmetric cut to the qualitatively equivalent multi-vortex setup in the two-dimensional NLSE. We would also like to compare the dynamics to the two-dimensional ordinary differential equations shown in Ref. [5] (which simulate vortex dynamics by treating the vortices as point sources), with the possibility of modifying them to accurately describe the three-dimensional axisymmetric vortex ring dynamics.

Numerous non-axisymmetric configurations are to be studied as well. One such scenario is when there are two opposite charge vortex rings approaching each other at an off-set to each other along the x or y direction. Depending on the amount they are off-center, one can see the rings merge, and then re-separate forming two new vortex rings traveling at an angle form the initial approach direction. The new rings have a quadrupole perturbation and exhibit breathing oscillations. We plan to track the deflection angle of the recombined rings and compare the angles to the off-set distance. In addition, we plan to vary the relative radii of the vortex rings and compare results. For the offset simulations, comparison to two-dimensional vortex dynamics can still be done as a two-dimensional cut along the off-set direction of the vortex rings looks qualitatively similar to four two-dimensional vortices (two of each charge) interacting. An example of an offset collision between two vortex rings is shown in Fig. 8.

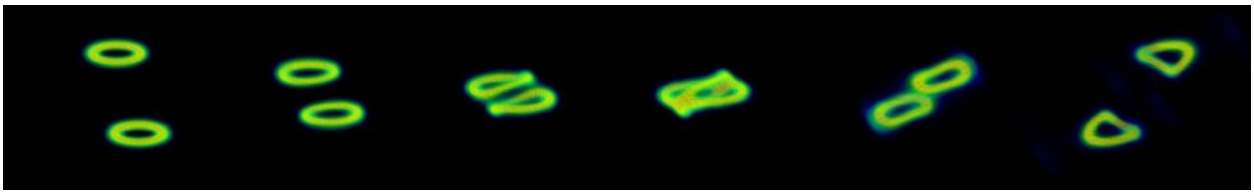

Figure 8: Example of off-set collision between two opposite unitary charge vortex rings.

Another non-axisymmetric configuration to be studied is two equal charge vortex rings side-by-side at different separation off-sets. These configurations yield interesting dynamics depending on the distance of the vortex rings. The rings start to rotate inward at an angle, which in turn causes them to travel towards each other until they merge. Then, it is predicted that depending on the distance, ring size, etc. the rings will either rotate together and detach, to be recombined in a flowing pattern, or the rings will stay merged and exhibit quadrupole oscillations. Additional variations include off-setting the rings in the z-axis as well, leading to further interesting dynamics to be explored.

As an extension to the previous configuration, we also study flowering patterns formed with a number of vortex rings of equal charge oriented in the x-y plane in cyclic-symmetric groups. For

example, arranging four vortex rings equally spaced from the origin in all four planar directions results in the rings combining and forming a small vortex ring with opposite charge (which shoots back on the opposite z-direction) and another large ring exhibiting oscillations. A similar configuration, but with an added fifth vortex ring in the center, yields an oscillating structure exhibiting a combining-detaching-recombining pattern of all rings.

Further configurations to be studied are vortex rings in chain-linked initial conditions at 90-degree orientation of each other (two rings in a similar scenario were studied in Ref. [40]). We will study large chain groups and chain rings consisting of multiple vortex rings linked into one large chain-ring. Also, overlapped vortex ring initial conditions will be studied. Preliminary simulations of two such rings has been done, showing the overlap portion of the rings become a new vortex ring of small radii, in which case has a larger velocity in the z-direction, and shoots past the leftover larger ring. Multiple overlapped vortex rings in a circular chain will also be simulated.

We expect that as the study progresses, additional interesting scenarios will present themselves and will be studied as well.

5 Overall Planning and Impact of Research Program

The proposed research plan is to be closely coordinated with Professor Ricardo Carretero, and is to take the expected duration of one year. The work will be mostly performed at the San Diego State University campus in the Computational Science Research Center Laboratory utilizing a high-end off-the-shelf GPU (Geforce GTX580) installed in a Windows 7 (Corei3) PC (both purchased with support from **NSF-DMS-0806762**). Previous work done at CGU is also implemented into the project, specifically the initial 3D MATLAB codes written under the advisement of the late Prof. Hedley Morris.

The following impacts of the study are relevant: 1) Thorough study of vortex ring dynamics in the NLSE will increase knowledge of the solutions and help understand more complicated and applied cases, most notably in BECs. 2) The numerical schemes formulated, including the MSD boundary condition, will help future researchers in their simulations of other systems governed by time-dependent complex PDEs. 3) Code packages including GPU-enabled routines provide other researchers interested in the NLSE with very valuable tools for three-dimensional simulations, which can be easily modified for specific applications (for example, simulating two-component BECs, altering the nonlinearity to be saturable for studies in nonlinear optics, etc). The codes also provide an excellent example in reproducibility of research, a topic of great interest to the computational science community. 4) The program is highly multidisciplinary, relying on knowledge and skills from physics, applied mathematics, numerical analysis, and computer science, making it a model project for the emerging field of computational science.

Selected Recent References by PI and advisor (related to proposed research)

[1] R. M. Caplan, Q. E. Hoq, R. Carretero-González, P. G. Kevrekidis. Azimuthal modulational instability of vortices in the nonlinear Schrödinger equation, Opt. Comm. **282** (2009) 1399–1405.

[2] R. M. Caplan. A Two-Step High Order Compact Scheme for the Laplacian Operator and its Implementation in a Fully Explicit Method for Integrating the Nonlinear Schrödinger Equation. In preparation to be submitted to Appl. Math and Comp., 2011.

[3] R. M. Caplan. A Simple Modulus-Squared Constant Background Dirichlet Boundary Condition for Time-Dependant Complex Partial Differential Equations and its Application to the Nonlinear Schrödinger Equation. In preparation to be submitted to Appl. Math and Comp., 2011.

[4] R. M. Caplan, R. Carretero-González, P. G. Kevrekidis, and B.A. Malomed. Existence, Stability, and Scattering of Bright Vortices in the Cubic-Quintic Nonlinear Schrödinger Equation. Submitted to Math. Comput. Simulat., 2010.

[5] P.T. Torres, R. Carretero-González, S. Middelkamp, P. Schmelcher, and P.G. Kevrekidis, D.J. Frantzeskakis. Vortex Interaction Dynamics in Trapped Bose-Einstein Condensates, To appear in Comm. Pure & Appl. Analysis, 2010.

[6] A.S. Rodrigues, P.G. Kevrekidis, R. Carretero-González, D.J. Frantzeskakis, P. Schmelcher, T.J. Alexander, and. Yu.S. Kivshar. Spinor Bose-Einstein condensate past an obstacle, Phys. Rev. A **79** (2009) 043603.

[7] R. Carretero-González, D.J. Frantzeskakis, and P.G. Kevrekidis, Nonlinear waves in Bose-Einstein condensates: physical relevance and mathematical techniques, Nonlinearity **21** (2008) R139–R202.

[8] R. Carretero-González, B. P. Anderson, P.G. Kevrekidis, D.J. Frantzeskakis, and N. Whitaker. Dynamics of vortex formation in merging Bose-Einstein condensate fragments. Phys. Rev. A **77** (2008) 033625.

[9] R. Carretero-González, N. Whitaker, P.G. Kevrekidis, and D.J. Frantzeskakis. Vortex structures formed by the interference of sliced condensates. Phys. Rev. A **77** (2008) 023605.

[10] P.G. Kevrekidis, R. Carretero-González, D.J. Frantzeskakis, and I.G. Kevrekidis. Vortices in Bose-Einstein Condensates: Some Recent Developments. Mod. Phys. Lett. B, **18** (2004) 1481–1505.

[11] P.G. Kevrekidis, D.J. Frantzeskakis, and R. Carretero-González. *Emergent Nonlinear Phenomena in Bose-Einstein Condensates: Theory and Experiment*. Springer Series on Atomic, Optical, and Plasma Physics, Vol. **45** (2008).

Other References

[12] L. Debnath. *Nonlinear Partial Differential Equations for Scientists and Engineers*, Birkhauser Second Edition (2005).

[13] T. Giamarchi, C. Rüegg, and O. Tchernyshyov. BoseEinstein condensation in magnetic insulators, Nat. Phys. **4** 3 (2008) 198–204

[14] H. Deng, H. Haug, and Y. Yamamoto. Exciton-polariton Bose-Einstein condensation, Rev. Mod. Phys. **82** 2 (2010) 1489–1537

[15] J. Klars, J. Schmitt, F. Vewinger, and M. Weitz. Bose-Einstein condensation of photons in a 'white-wall' photon box, J. Phys. Conf. **264** (2011) 012005

[16] H. Saito, and M. Ueda. Mean-field analysis of collapsing and exploding Bose-Einstein condensates, Phys. Rev. A **65** (2002) 033624.

[17] S. Wuster, J. J. Hope, and C. M. Savage. Collapsing Bose-Einstein condensates beyond the Gross-Pitaevskii approximation, Phys. Rev. A **71** (2005) 033604.

[18] F. Dalfovo, S. Giorgini, L. P. Pitaevskii, and S. Stringari. Theory of Bose-Einstein condensation in trapped gases, Rev. Mod. Phys. **71** 3 (1999) 463–512.

[19] B.A. Malomed. Variational methods in nonlinear fiber-optics and related fields, Prog. Opt. **43** (2002) 71–193.

[20] B. P. Anderson. Resource Article: Experiments with Vortices in Superfluid Atomic Gases, J. Low Temp. Phys. **161** 5-6 (2010) 574–602.

[21] P. H. Roberts and J. Grant. Motions in a Bose condensate. I. The structure of the large circular vortex, J. Phys. A: Gen. Phys. **4** (1971) 55.

[22] G. W. Rayfield and F. Reif. Quantized Vortex rings in Superfluid Helium, Phys. Rev. **136** 5A (1964) A1194–A1208.

[23] B. P. Anderson, P. C. Haljan, C. A. Regal, D. L. Feder, L. A. Collins, C.W. Clark, and E. A. Cornell. Watching Dark Solitons Decay into Vortex Rings in a Bose-Einstein Condensate, Phys. Rev. Lett. **86** 14 (2001) 2926–2929.

[24] I. Shomroni, E. Lahoud, S. Levy and J. Steinhauer. Evidence for an oscillating soliton/vortex ring by density engineering of a Bose-Einstein condensate, Nat. Phys. Lett. **5** (2009) 193–197.

[25] J. Ruostekoski and Z. Dutton. Engineering vortex rings and systems for controlled studies of vortex interactions in Bose-Einstein condensates, Phys. Rev. A **72** (2005) 063626. 0

[26] J. Ruostekoski and J. R. Anglin. Creating Vortex Rings and Three-Dimensional Skyrmions in Bose-Einstein Condensates, Phys. Rev. Lett. **86** 18 (2001) 3934–3937.

[27] N. G. Berloff and C. F. Barenghi. Vortex Nucleation by Collapsing Bubbles in Bose-Einstein Condensates, Phys. Rev. Lett. **93** 9 (2004) 090401.

[28] N. G. Berloff. Evolution of rarefaction pulses into vortex rings, Phys. Rev. B **65** (2002) 174518.

[29] N. G. Berloff. Vortex nucleation by a moving ion in a Bose condensate, Phys. Lett. A **277** 9 (2000) 240–244.

[30] B. Jackson, J. F. McCann, and C. S. Adams. Vortex rings and mutual drag in trapped Bose-Einstein condensates, Phys. Rev. A **60** 6 (1999) 4882–4885.

[31] D. Amit, and E. P. Gross. Vortex Rings in a Bose Fluid, Phys. Rev. **145** 1 (1966) 130–136.

[32] M. Abad, M. Guilleumas, R. Mayol, and M. Pi. Vortex Rings in Toroidal BoseEinstein Condensates, Las. Phys. **18** 5 (2008) 648–652.

[33] C. H. Hsueh, S. C. Gou, T. L. Horng, and Y. M. Kao. Vortex-ring solutions of the GrossPitaevskii equation for an axisymmtrically trapped BoseEinstein condensate, J. Phys. B: At. Mol. Opt. Phys. **40** (2007) 4561-4571.

[34] M. Guilleumas, D. M. Jezek, R. Mayol, M. Pi, and M. Barranco1. Generating vortex rings in Bose-Einstein condensates in the line-source approximation, Phys. Rev. A **65** (2002) 053609.

[35] L.-C. Crasovan, V. M. Pérez-Gárcía, I. Danaila, D. Mihalache, and L. Torner. Three-dimensional parallel vortex rings in Bose-Einstein condensates, Phys. Rev. A **70** (2004) 033605.

[36] T. L. Horng, S. C. Gou, and T. C. Lin. Bending-wave instability of a vortex ring in a trapped Bose-Einstein condensate, Phys. Rev. A **74** (2006) 041603(R).

[37] T.-L. Horng, C.-H. Hsueh, and S.-C. Gou. Transition to quantum turbulence in a Bose-Einstein condensate through the bending-wave instability of a single-vortex ring, Phys. Rev. A **77** (2008) 063625.

[38] B. Jackson, J. F. McCann, and C. S. Adams. Vortex line and ring dynamics in trapped Bose-Einstein condensates, Phys. Rev. A **61** (1999) 013604.

[39] S. Komineas and J. Brand. Collisions of Solitons and Vortex Rings in Cylindrical Bose-Einstein Condensates, Phys. Rev. Lett. **95** (2005) 110401.

[40] J. Koplik and H. Levine. Scattering of Superfluid Vortex Rings, Phys. Rev. Lett. **76** 25 (1996) 4745–4748.

[41] P. Engels. Viewpoint: Observing the dance of a vortex–antivortex pair, step by step, Physics **3** 33 (2010).

[42] J. Belmonte. E-mail Correspondence.

[43] W. F. Spotz and G. F. Carey. Iterative and Parallel Performance of High-Order Compact Systems, SIAM J. Sci. Comput. **19** 1 (1998) 1–14.

[44] W. Liao. An implicit fourth-order compact finite difference scheme for one-dimensional Burgers' equation, Appl. Math. and Comp. **206** (2008) 755–764.

[45] W. F. Spotz and G. F. Carey. A High-Order Compact Formulation for the 3D Poisson Equation, Num. Meth. for Par. Diff. Equ. **12** (1996) 235–243.

[46] J. Zhang. An explicit fourth-order compact finite difference scheme for three-dimensional convection-diffusion equation, Comm. Num. Meth. for Engn. **14** (1998) 209–213.

[47] L. Ge and J. Zhang. Symbolic computation of high order compact difference schemes for three dimensional linear elliptic partial differential equations with variable coefficients, J. Comp. Appl. Math. **143** 1 (2002) 9–27.

[48] W. F. Spotz and G. F. Carey. Extension of High-Order Compact Schemes to Time-Dependent Problems, Num. Meth. for Par. Diff. Equ. **17** 6 (2001) 657–672.

[49] M. Ciment and S. H. Leventhal. Higher Order compact Implicit Schemes for the Wave Equation, Math. Comp. **29** 132 (1975) 985–994.

[50] S. Xie, G. Li, and S. Yi. Compact finite-difference schemes with high accuracy for one-dimensional nonlinear Schrödinger equation, Comp. Meth. Appl. Mech. Engi. **198** (2009) 1052–1060.

[51] M. Dehghan and A. Taleei. A compact split-step finite difference method for solving the nonlinear Schrödinger equations with constant and variable coefficients, Comp. Phys. Comm. **181** (2010) 43–51.

[52] A. Mohebbi, and M. Dehghan. The use of compact boundary value method for the solution of two-dimensional Schrodinger equation, J. Comp. Appl. Math. **225** (2009) 124–134.

[53] J. C. Kalita, P. Chhabra, and S. Kumar. A semi-discrete higher order compact scheme for the unsteady two-dimensional Schrdinger equation, J. Comp. Appl. Math. **197** (2006) 141–149.

[54] J. C. Strikwerda. *Finite Difference Schemes and Partial Differential Equations*, SIAM Second Edition (2004).

[55] M. S. Ismail. A fourth-order explicit schemes for the coupled nonlinear Schrödinger equation, Appl. Math. and Comp. **196** (2008) 273–284.

[56] Nvidia Corp. Whitepeper, NVIDIAs Next Generation CUDA Compute Architecture: Fermi (2009).

[57] K. Karimi, N. G. Dickson, and F. Hamze. A Performance Comparison of CUDA and OpenCL, arXiv:1005.2581 (2010).

[58] K.A. Hawick and D. P. Playne. Numerical Simulation of the Complex Ginzburg-Landau Equation on GPUs with CUDA, Submitted to: Parallel Dist. Comp. Net. (PDCN 2011), `http://www.massey.ac.nz/~dpplayne/Papers/cstn-070.pdf`

[59] P. Micikevicius. 3D finite difference computation on GPUs using CUDA, Proceedings of 2nd Workshop on General Purpose Processing on Graphics Processing Units, (2009) 79–84.

[60] D. Michéa and D. Komatitsch. Accelerating a three-dimensional finite-difference wave propagation code using GPU graphics cards, Geo. J. Inter. **182** 1 (2010) 389-402

[61] S. Adams and J. Payne. Finite Difference Time Domain (FDTD) Simulations Using Graphics Processors, HPCMP Usr. Grp. Conf. (2007) 0-7695-3088-5/07.

[62] J. Nocedal and S. J. Wright. Numerical Optimization, Springer, Second Edition, (2006).

[63] D. L. Donoho, A. Maleki, I. U. Rahman, M. Shahram, and V. Stodden. Reproducible Research in Computational Harmonic Analysis, Comp. Sci. Engi. **11** 1 (2009) 8–18.